ARTICLE OPEN

Check for updates

MYELODYSPLASTIC NEOPLASM

CRISPR-engineered human GATA2 deficiency model uncovers mitotic dysfunction and premature aging in HSPCs, impairing hematopoietic fitness

Damia Romero-Moya[1], Eric Torralba-Sales[1], Cristina Calvo[2,3], Oskar Marin-Bejar[1,4], Maria Magallon-Mosella[1], Maximiliano Distefano[5], Joan Pera[1], Julio Castaño[6], Francesca De Giorgio[1], Jessica Gonzalez[7,8,9], Arnau Iglesias[7,8,9], Clara Berenguer-Balaguer[10], Marcel Schilling[11,17], Mireya Plass[11,12], Lorenzo Pasquali[10], Albert Català[5,13], Oscar Molina[2,3], Marcin W. Wlodarski[14], Anna Bigas[7,8,9] and Alessandra Giorgetti[1,15,16]✉

GATA2 deficiency is a monogenic transcriptopathy disorder characterized by bone marrow failure (BMF), immunodeficiency, and a high risk of developing myelodysplastic neoplasms (MDS) and acute myeloid leukemia (AML). Although informative mouse models have been developed, the mechanisms by which GATA2 haploinsufficiency drives disease initiation in humans remain incompletely understood. To address this, we developed a novel humanized model using CRISPR/Cas9 technology to knock-in GATA2-R398W variant in primary cord blood CD34⁺ cells. Additionally, we introduced specific mutations in SETBP1 and ASXL1 to model distinct premalignant stages of GATA2 deficiency. Through clonal competition and serial transplantation assays, we demonstrated that human CD34⁺ cells harboring the GATA2 mutation exhibit significantly reduced fitness in vivo when compete with wild-type cells. Notably, this fitness disadvantage persists even when GATA2 mutations are combined with oncogenic SETBP1 and ASXL1 drivers, underscoring the dominant, deleterious effect of GATA2 deficiency on hematopoietic stem cell function. Functional in vitro analyses revealed that GATA2-R398W mutation impairs cell proliferation, disrupts cell cycle progression, and induces mitotic defects, which may contribute to hematopoietic stem/progenitor cell loss and impaired self-renewal. Transcriptomic profiles of GATA2-mutant cells revealed that these functional defects are associated with reduced HSC self-renewal capacity and upregulation of the pre-aging phenotype. Our work highlights the feasibility of generating a human GATA2 deficiency model suitable for studying the biological consequences of various GATA2 variants and the generation of a platform to test potential phenotype-rescuing therapeutics.

Leukemia (2025) 39:3015–3025; https://doi.org/10.1038/s41375-025-02771-8

INTRODUCTION

GATA2 is a transcription factor required for the generation and survival of hematopoietic stem and progenitor cells (HSPCs) [1]. In humans, heterozygous germline GATA2 mutations cause hematologic, immunologic and vascular disorders, collectively known as GATA2 deficiency [2–5]. The patients suffer of immunodeficiency, bone marrow failure (BMF), and high propensity to develop myelodysplastic neoplasms (MDS) and acute myeloid leukemia (AML), with the median age at diagnosis estimated at 17–21 years [6, 7]. The mutational landscape of GATA2 deficiency continues to expand, comprising 850 published cases with 230 distinct familial or de novo germline GATA2 mutations [2–15]. These mutations

[1]Regenerative Medicine Program, Institut d'Investigació Biomèdica de Bellvitge (IDIBELL), Barcelona, Spain. [2]Department of Physiological Sciences, Genetics Section, School Of Medicine, University of Barcelona, L'Hospitalet de Llobregat, Spain. [3]Josep Carreras Leukaemia Research Institute, School of Medicine, University of Barcelona, Barcelona, Spain. [4]Germans Trias i Pujol Health Science Research Institute (IGTP), Cancer Program, Badalona, Catalonia, Spain. [5]Department of Hematology and Oncology, Institut de Recerca Sant Joan de Déu, Hospital Sant Joan de Deu, Barcelona, Spain. [6]Hospital Sant Joan de Deu Advanced Therapies Platform, SJD Pediatric Cancer Center Barcelona (PCCB) building, Barcelona, Spain. [7]Centro de Investigación Biomédica en Red de Oncología (CIBERONC), Instituto de Salud Carlos III, Madrid, Spain. [8]Programa de Investigación en Cáncer, IMIM (Hospital del Mar Medical Research Institute), Barcelona, Spain. [9]Josep Carreras Leukemia Research Institute (IJC), Badalona, Spain. [10]Department of Medicine and Life Sciences, Endocrine Regulatory Genomics, Universitat Pompeu Fabra (UPF), Barcelona, Spain. [11]Gene Regulation of Cell Identity Lab, Neurosciences Program, Bellvitge Institute for Biomedical Research (IDIBELL), L'Hospitalet del Llobregat, Spain. [12]Physiological Sciences Department, Faculty of Medicine and Health Sciences, University of Barcelona, L'Hospitalet del Llobregat, Spain. [13]Instituto de Salud Carlos III, Biomedical Network Research Centre on Rare Diseases, Madrid, Spain. [14]Department of Hematology, St. Jude Children's Research Hospital, Memphis, TN, USA. [15]Department of Pathology and Experimental Therapeutics, Faculty of Medicine and Health Sciences, Barcelona University, Barcelona, Spain. [16]Center for Networked Biomedical Research on Bioengineering, Biomaterials and Nanomedicine (CIBER-BBN), Madrid, Spain. [17]Present address: Department of Genetics, Microbiology and Statistics, Faculty of Biology, University of Barcelona, Barcelona, Spain. ✉email: agiorgetti@idibell.cat

Received: 5 August 2025 Revised: 20 August 2025 Accepted: 8 September 2025
Published online: 15 September 2025

can be categorized into four major types: truncating mutations, missense mutations (predominantly in zinc finger domain 2, ZF2), noncoding mutations disrupting the auto-enhancer site in intron 4, and synonymous mutations causing monoallelic RNA degradation [11]. Missense mutations impair DNA binding capability, whereas others act through haploinsufficiency mechanisms [2, 3, 16, 17]. MDS and leukemia arise as secondary events in GATA2 carriers and are usually associated with the acquisition of somatic or cytogenetic alterations. Monosomy 7 [6] and somatic mutations in *SETBP1* and *ASXL1* genes are common in GATA2-related pediatric MDS patients [7–9, 15, 18]. Zebrafish and mouse models have been used to study GATA2 haploinsufficiency. In zebrafish, Gata2a$^{-/-}$ mutants display deficient marrow with hypocellularity and neutropenia while maintaining erythropoiesis [19, 20], on the other hand Gata2b$^{+/-}$ show reduced HSPC function with impaired myeloid differentiation [21–23]. Gata2$^{+/-}$ mice showed a reduction in HSC number and lower functionality [24–29]. Other studies based on the ablation of the upstream Gata2-77 enhancer demonstrated abrogation of the multilineage differentiation potential of fetal liver progenitors' cells without affecting HSC emergence, which is diminished by the intronic +9.5 enhancer deletion [26, 30–32]. Recent studies report that GATA2 haploinsufficiency results in lethal BMF and leukemia progression after serial transplantation, likely due to proliferative defects and genomic instability [29]. In addition, mouse models with missense mutation in the ZF2 (L359V, R396Q, and R398W) have been developed [17, 33–35]. Mouse models carrying the R396Q mutation exhibit loss of stemness, myeloid bias, and premature aging [34, 35], while the R398W mutation impairs DNA binding and induces dendritic cell, monocyte B and NK lymphoid (DCML)-like phenotype [17].

While these models have significantly advanced our understanding of how GATA2 mutations impair hematopoiesis, they fail to accurately replicate the hematological phenotype observed in patients. Additionally, GATA2-deficient models using patient-derived [36] or CRISPR/Cas9-edited induced pluripotent stem cells iPSCs [37] show only a mild hematopoietic defect. Finally, the challenges associated with patient-derived xenograft from MDS cells, including those from GATA2 carriers, underscoring the need for physiologically relevant systems. CRISPR/Cas9-engineered human cord blood (CB) CD34$^+$ HSPCs offer a promising alternative, with high engraftment potential and preserved long-term repopulation.

Here, we developed a novel human model by introducing GATA2-R398W, SETBP1, and ASXL1 mutations into CB CD34$^+$ cells using CRISPR/Cas9. This approach mimics the mutational landscape observed in pediatric GATA2-related MDS patients [15] and provides a unique platform to investigate the functional and cooperative effects of these mutations in a human context.

METHODS

CD34$^+$ HSPCs culture

Frozen or freshly purified CD34$^+$ cells were prestimulated for 24–48 h before nucleofection on SFM StemPro-34 + 1%P/S + 1%Glu (Gibco; Waltham, MA, USA) supplemented with early hematopoietic cytokines. Cell incubation conditions were maintained 37 °C, 5% CO_2 and 20% O_2 for the liquid culture conditions.

Genome editing of CD34$^+$ HSPCs

Chemically modified Alt-R CRISPR-Cas9 sgRNAs and Alt-R S.p.HiFi Cas9 Nuclease V3 (IDT), were used to edit CD34$^+$ cells at *GATA2*, *SETBP1*, and *ASXL1*. RNPs were complexed with 100 pmol of HiFi Cas9 and 120 pmol of sgRNA at 25 °C for 10 min before electroporation with the 4D-Nucelofector (Program DZ-100; Lonza; Basel, Switzerland). Immediately after the nucleofection, rAAV6 was supplied to the cells at 2×10^4 vector genomes per cell for overnight incubation. For control condition, 5×10^5 cells were nucleofected without RNP complex.

Mice transplantation and follow-up

NOD-*scid* IL2Rg^{null}mice (NSG; $n = 38$) were used for primary transplantation and NOD-*scid* IL2Rg^{null}-3/GM/SF (NSG-S; $n = 30$) were used for secondary transplantation, which improves multilineage hematopoietic reconstitution. For primary transplantation between 1×10^5 and 3×10^5 unsorted HSPCs (control, GATA2 and multiplex conditions) were intra BM transplanted (IBMT) four days after nucleofection. Peripheral blood (PB) was analyzed periodically until they reached the end point (16-weeks). In the secondaries at least 2×10^6 BM cells were injected into recipients, animals were bled periodically until the end point (24-weeks).

Statistical analysis

Unless otherwise specified, the Student's *t* test and one-way ANOVA was applied for variables that meet normality assumptions, while the Mann–Whitney U test or Kruskal-Wallis test was used for non-normally distributed variables. Statistical analyses were performed with GraphPad Prism v9.1.

RESULTS

In vivo engraftment of multiplex-engineered CD34$^+$ cells

While germline GATA2 mutations have been studied in animal models, their effects in human HSPCs remain unclear. Disease progression often involves secondary mutations (e.g., SETBP1, ASXL1), whose roles are not yet defined. To investigate the effect of these mutations, we utilized multiplex CRISPR/Cas9 genome editing in CB CD34$^+$ cells, followed by competitive serial transplantation assays (Fig. 1A). To maximize homologous recombination (HR) and enable tracking of cells edited for GATA2-R398W, we combined the CRISPR/Cas9 with recombinant adeno-associated virus serotype 6 (rAAV6) for donor template delivery. The single-stranded AAV6 donor was designed with homology arms targeting *GATA2* exon 6 and incorporated (i) the clinically relevant GATA2 c.1192 C > T (p.R398W) mutation, along with silent SNPs to prevent Cas9 re-cutting, and (ii) an in frame green fluorescent protein (GFP) cassette to enable efficient selection and tracking of edited cells. For hotspot leukemia driver mutations SETBP1 (c.2602 G > A; D868N) and ASXL1 (c.1934dupG; G646Xfs*12), single-stranded oligodeoxynucleotides (ssODNs) served as donor templates (Fig. 1A). Three experimental conditions were assessed [1]: Control: Mock-unedited CD34$^+$ cells [2], GATA2: cells edited with GATA2-R398W mutation, and [3] Multiplex: cells simultaneously edited for *GATA2*, *SETBP1*, and *ASXL1* (Fig. 1A). Four days after nucleofection, flow cytometry analysis of GFP$^+$ cells revealed average HR efficiencies of 10% for GATA2 and 5% for multiplex condition (Fig. 1B). To assess the efficiency of gene targeting in CB CD34$^+$ cells, we performed colony-forming unit (CFU) assays using GFP$^+$ and GFP$^-$ sorted cells from both GATA2 and multiplex conditions, followed by genomic analysis of single-cell-derived colonies. In the GATA2 condition, 74% of colonies derived from GFP$^+$ cells carried the GATA2-R398W mutation in a monoallelic state, and 26% showed biallelic editing. In contrast, 44% of colonies derived from GFP$^-$ cells harbored indels. In the multiplex condition we detected mutations across all the three targeted genes, with *SETBP1* being the most frequently edited (Fig. 1C). Genomic analysis of colonies generated from GFP$^+$ cells revealed a strong enrichment for dual and triple gene editing: 69% carried mutations in both *SETBP1* and *GATA2*-R398W, while 12.5% showed simultaneous targeting of *SETBP1*, *ASXL1*, and *GATA2*-R398W in heterozygous. These results demonstrate the high efficiency of our multiplex CRISPR/Cas9 strategy, enabling functional modeling of GATA2 deficiency in a human context.

Next, we assessed engraftment using multiclonal competition assays by transplanting unsorted GATA2 and multiplex-edited cells into NSG mice (Fig. 1A, total mice $n = 38$). Notably, our transplantation model serves as a competitive assay where wild-type cells, GATA2-mutant cells, and cells harboring oncogenic somatic mutations compete within the same environment. Flow

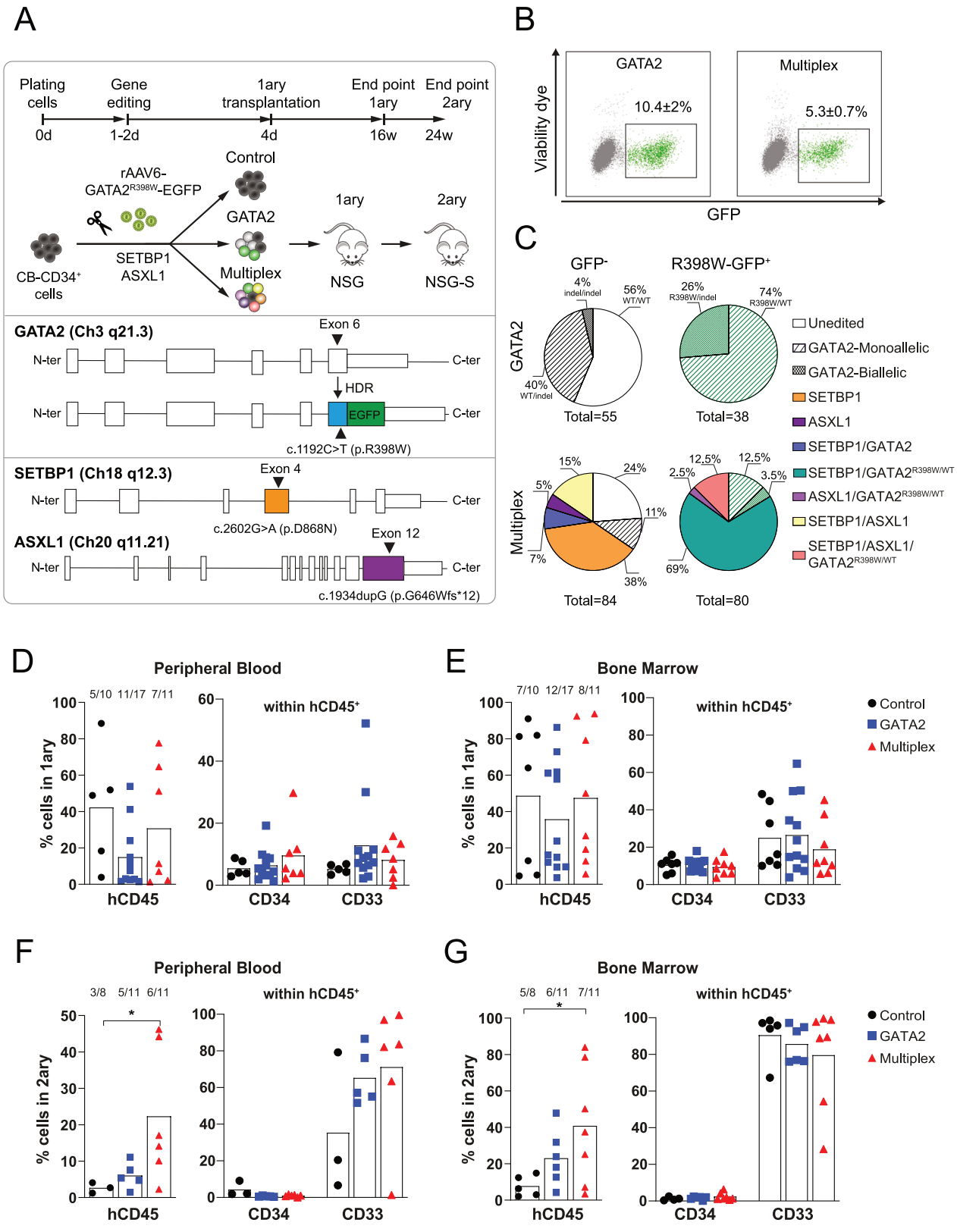

cytometry analysis (Fig. S1A) at 16 weeks post-transplantation revealed more than 10% of human cell engraftment in PB and 20% in BM (Fig. 1D, E; Fig. S1B) for all conditions. Moreover, multilineage reconstitution was observed without significant bias across the different conditions (Fig. 1D, E). To study long-term clonal evolution, we performed secondary transplants in NSG-S mice. At 24 weeks 18 out of 30 mice showed >1% in BM engraftment. PB flow cytometry analysis revealed that a subset of mice in the multiplex condition exhibited a significant increase in hCD45^{+} cell engraftment (6%) compared to control (1%) and

Fig. 1 Multiplex CRISPR/Cas9 allows the introduction of multiple GATA2, SETBP1 and ASXL1 mutations. A Schematic representation of the experimental workflow. Control condition: unedited cord blood-derived $CD34^+$ (CB-$CD34^+$) cells. GATA2 condition: CB-$CD34^+$ cells edited to introduce the $GATA2^{R398W}$ mutation via CRISPR/Cas9 and rAAV6-$GATA2^{R398W}$-EGFP template delivery. Multiplex condition: simultaneous editing of *GATA2*^{R398W}, *SETBP1*, and *ASXL1* using CRISPR/Cas9 and rAAV6-$GATA2^{R398W}$-EGFP. Four days post-nucleofection, edited and unedited cells from all conditions were transplanted into primary NSG mice for 16 weeks. Secondary transplantation was performed in NSG-S mice for an additional 24 weeks. Schematic illustration of the edited genes. In GATA2, the exon 6 has been modified with silent single nucleotide polymorphisms (SNPs), and the EGFP is introduced in-frame immediately following exon 6. The SETBP1 donor introduces the c.2602 G > A (D868N) mutation, and the ASXL1 donor introduces the c.1934dupG (G646Wfs*12) mutation. **B** Percentage of GFP^+ cells four days after nucleofection showing the efficiency of GATA2 editing (GATA2-R398W-EGFP) ($n \geq 10$). **C** Pie plots summarizing the results of targeted DNA sequencing for *GATA2*, *SETBP1*, and *ASXL1* genes across four conditions: GATA2-GFP^+, GATA2-GFP^-, multiplex-GFP^+, and multiplex-GFP^-. Data was obtained from isolated colonies cultured in methylcellulose for 14 days ($n \geq 8$). **D** Peripheral blood (PB) human chimerism ($hCD45^+ > 1\%$) of the primary mice at the 16-week endpoint. The data includes the number of engrafted mice and the distribution of $CD34^+$ and $CD33^+$ cells within the $hCD45^+$ population in PB. **E** Bone marrow (BM) human chimerism ($hCD45^+ > 1\%$) of the primary mice at the 16-week endpoint. The data includes the number of engrafted mice and the distribution of $CD34^+$ and $CD33^+$ cells within the $hCD45^+$ population in PB. **F** PB human chimerism ($hCD45^+ > 1\%$) of the secondary mice at the 24-week endpoint. The data includes the number of engrafted mice and the distribution of $CD34^+$ and $CD33^+$ cells within the $hCD45^+$ population in PB; Student's *t* test. **G** BM human chimerism ($hCD45^+ > 1\%$) of the secondary mice at the 24-week endpoint. The data includes the number of engrafted mice and the distribution of $CD34^+$ and $CD33^+$ cells within the $hCD45^+$ population in PB; Student's *t* test. *$p < 0.05$.

GATA2 (2%) (Fig. S1C). By 24 weeks, the average percentage of $hCD45^+$ cells in PB reached 26% in the multiplex condition, compared to 3% and 6% in the control and GATA2 conditions, respectively (Fig. 1F; Fig. S1C). This trend persisted in the BM, where engraftment levels remained higher in the multiplex condition compared to the control and GATA2 groups (Fig. 1G). Flow cytometry analysis revealed a predominantly myeloid profile ($CD33^+$), consistent with the mouse strain used (Fig. 1G), with no differences in monocytes ($CD14^+$) or granulocytes ($CD15^+$) subpopulations across conditions (Fig. S1D). In summary, these data demonstrate that multiplex gene editing of human CB $CD34^+$ cells targeting the *GATA2*, *SETBP1*, and *ASXL1* genes is feasible and does not compromise engraftment potential.

Clonal dynamics reveal that GATA2 mutation impairs HSPC fitness in vivo

To dissect the clonal architecture of human engrafted cells, we assessed GFP^+ cells by flow cytometry and performed deeper genomic studies of BM engrafted $hCD45^+$ cells of primary and secondary mice ($hCD45^+ > 1\%$). Primary mice exhibited low GFP^+ percentage (0.02–1.6%) in both GATA2 and multiplex conditions (Fig. S2A), which disappeared in the corresponding secondary recipients. Since the decrease in GFP expression could reflect downregulation of GATA2 expression, to detect GATA2-R398W and related indels, we performed genomic analysis of sorted $hCD45^+$ cells s from primary and secondary BM. Of 102 single-cell-derived colonies analyzed from eight different primary mice under the GATA2 condition, only 4 colonies (4%) harbored a heterozygous GATA2-R398W mutation, while 28% (3% homozygous and 26% heterozygous) of the colonies carried indels. Additionally, whole exome sequencing (WES) and DNA sanger analysis of sorted bulk $hCD45^+$ cells revealed that in the GATA2 condition only 1 out of 6 secondary mice showed the presence of indels in the *GATA2* locus (Fig. 2A; Table S1), which likely explains why engraftment levels in the GATA2 group were comparable to those in control (Fig. 1F, G). Specifically, primary mouse #57656 harbored six distinct indels at the *GATA2* locus, with a cumulative variant allele frequency (VAF) of 17%. However, after secondary transplantation into two mice, only one mouse maintained a clone carrying the likely pathogenic L399fs mutation (Fig. 2A; Table S1). These data suggest that, in a competitive setting with wild-type cells, GATA2-mutant cells declined over the first 4 months post-transplantation. A similar trend was observed for the multiplex condition. Genomic analysis of $hCD45^+$ single-cell-derived colonies from primary mice (#28344 and #23339) revealed no detectable *GATA2* mutations. In contrast, the predominant expanded clones carried either *SETBP1* mutations alone or co-occurring *SETBP1* and *ASXL1* mutations (Fig. 2B; Fig. S2B; Table S1). These findings were further validated by WES, which consistently identified *SETBP1* and *ASXL1* as the dominant mutations within the most competitive clones (Fig. 2C, D; Fig. S2C, D; Table S1). Notably, primary mouse #22984 harbored multiple mutations across *GATA2*, *SETBP1*, and *ASXL1*; however, only clones with double *SETBP1* and *ASXL1* mutations expanded in the secondary recipients (Fig. 2C; Fig. S2C; Table S1), further supporting the enhanced fitness conferred by these oncogenic drivers. This clonal advantage was reflected in the high levels of human BM engraftment observed in mice #53070 and #39249, both exceeding 50% (Fig. S1E; Table S1). Overall, the lack of expansion of GATA2-mutant clones in this competitive setting aligns with previous reports [25, 28, 35], reinforcing the concept that GATA2 mutations impair HSC fitness.

GATA2-R398W mutation induced cell cycle arrest and mitotic defects in $CD34^+$ cells

To better understand the in vivo disadvantage of GATA2-mutant cells, we conducted deeper functional in vitro assays. We FACS-sorted three populations: GFP^+ (R398W-mutant), GFP^- (they could contain either wild-type cell or with indels in *GATA2*, as described in Fig. 1C), and control cells (Fig. 3A). In liquid culture, GFP^+ cells from both GATA2 and multiplex conditions exhibited a marked proliferation defect emerging at day 10 when compared with GFP^- and control cells, leading to near depletion by third week (Fig. 3B). Consistently, GFP^+ HSPCs displayed a marked reduction in the total number of colonies compared to their GFP^- counterparts and controls, indicating impaired clonogenic potential (Fig. 3C; Fig. S3A). To assess the temporal dynamics of mutant clones, cells were seeded at different time points during liquid culture (days 0, 7, and 14), and colonies were counted. Notably, colonies derived from GATA2-R398W-mutant cells declined over time and disappeared earlier than controls, further indicating reduced proliferative capacity and fitness (Fig. S3B). Longitudinal analysis of single-cell-derived colonies showed loss of GATA2 biallelic mutants by day 7, confirming the essential role of GATA2 and the unviability of complete knockout in HSPCs (Fig. S3C). Based on these data, all functional analysis were performed starting on day 10 of culture, ensuring that our findings reflect GATA2 haploinsufficiency rather than mixed-population effects. Flow cytometry analysis revealed a marked reduction in $CD34^+$ cells within the GFP^+ population when compared with GFP^- and control cells (Fig. 3D). This decline was associated with a reduction in the G2/S/M cell cycle phases rather than apoptosis rates, suggesting impaired self-renewal capacity in GATA2-mutant cells (Fig. 3E, F). Consistent with the observed defects in proliferation and stemness, mitotic analysis of GFP^+ cells revealed a significantly reduced mitotic index, as observed by the rates of mitotic cells compared with controls, indicating impaired cell cycle progression

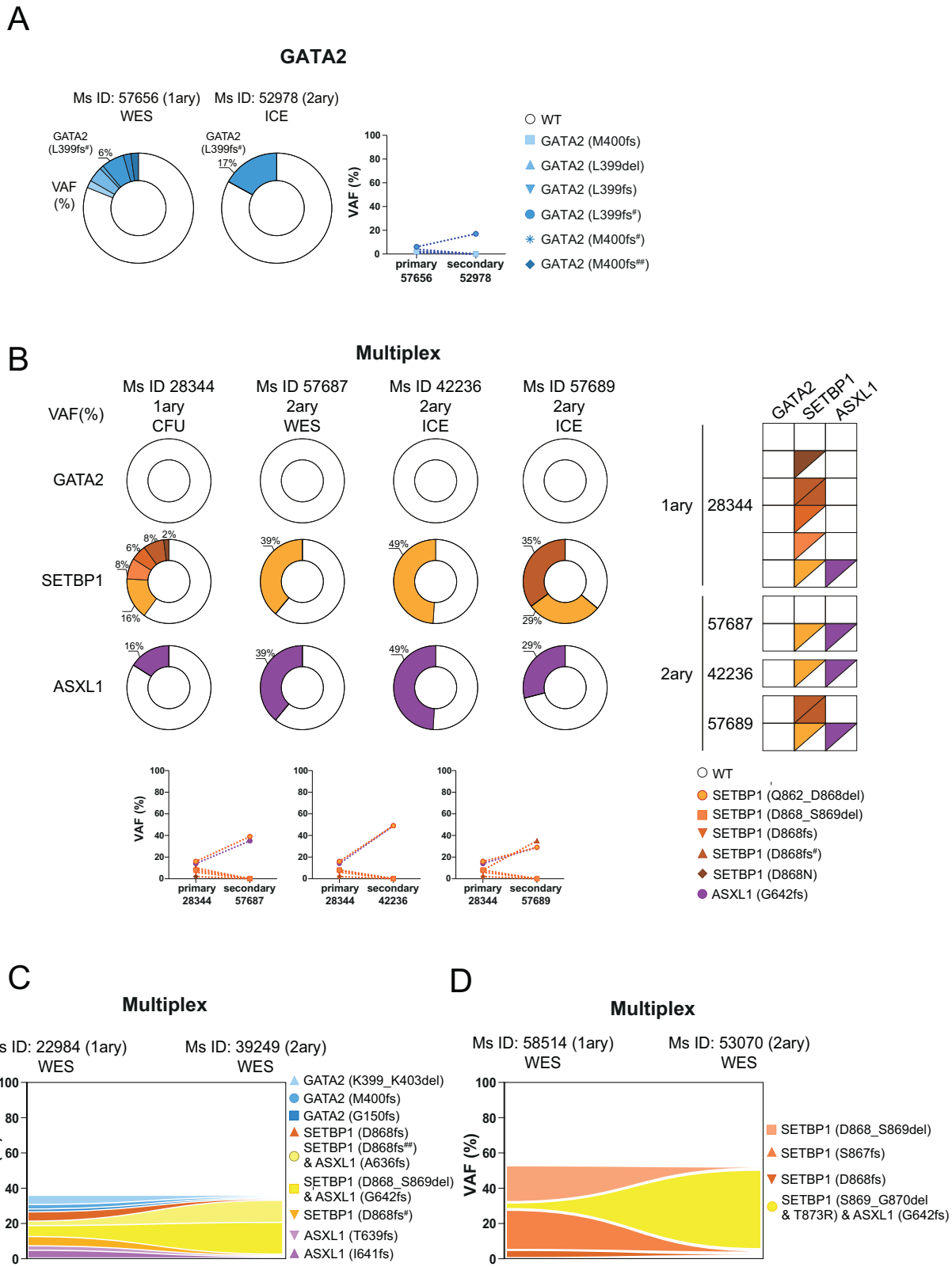

Fig. 2 GATA2-mutant cells have disadvantage in an in vivo clonal competition model. A The percentage of variant allele frequency (VAF) in primary and secondary GATA2 recipients are visualized using pie charts. Allelic distribution was analyzed through whole exome sequencing (WES), and Sanger sequencing combined with ICE software analysis (ICE). **B** The percentage of VAF in primary and secondary multiplex recipients are visualized using pie charts. Allelic distribution was analyzed through single clone genotyping (CFU), WES, and Sanger sequencing combined with ICE. Squares with triangles denote the distinct clones identified in the analysis. **C** The percentage of VAF and clonal dynamics in primary and secondary multiplex recipients are visualized using fish plot formats. Allelic distribution was analyzed by WES. **D** The percentage of VAF and clonal dynamics in primary and secondary multiplex recipients are visualized using fish plot formats. Allelic distribution was analyzed by WES.

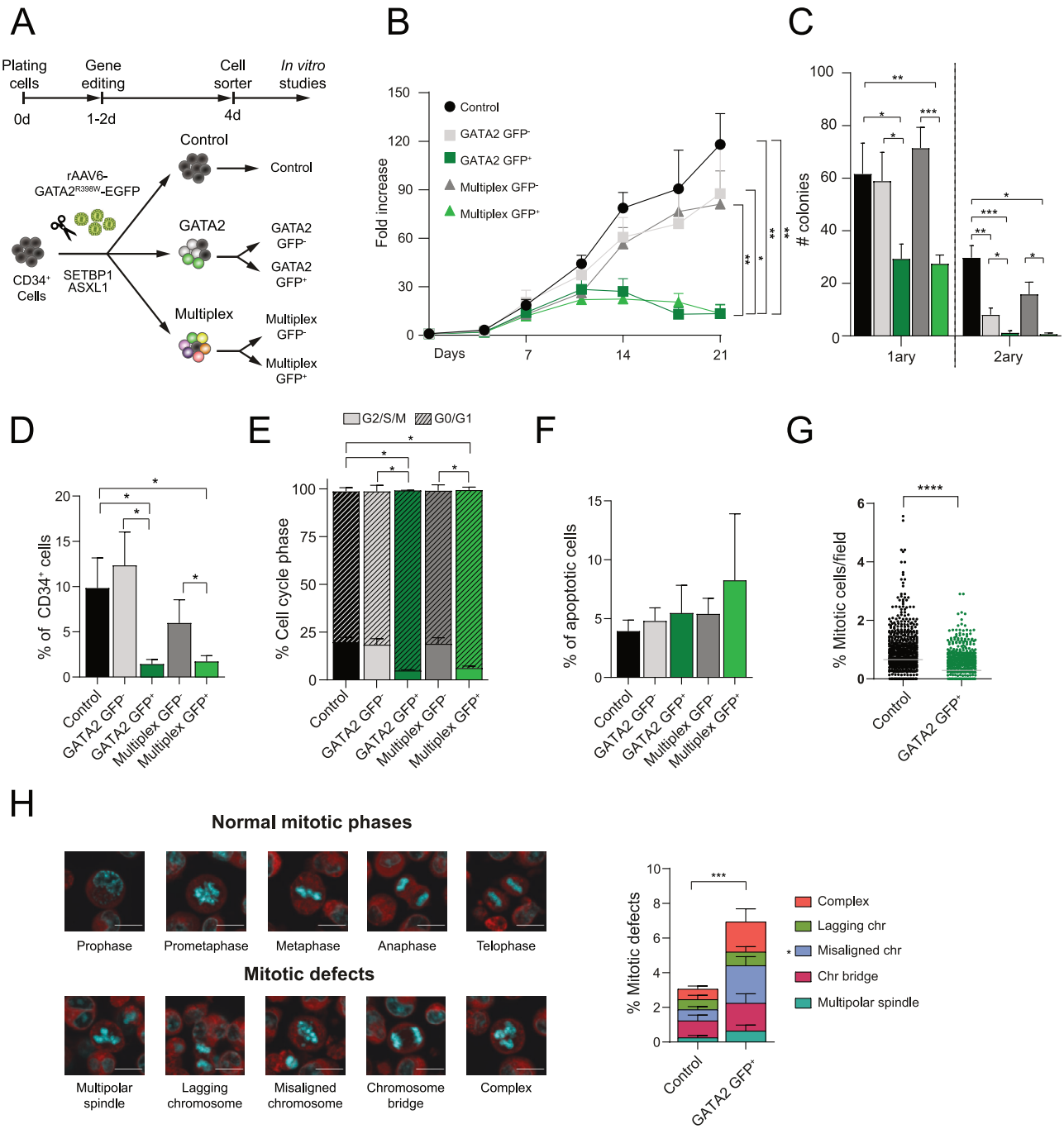

Fig. 3 GATA2 mutation impairs proliferation and clonogenic capacity in vitro. A Schematic representation of the in vitro experimental design. GATA2 condition: The GATA2-R398W mutation was introduced into CD34$^+$ cells using CRISPR/Cas9 combined with rAAV6-GATA2^{R398W}-EGFP for template delivery. Multiplex condition: Multiple simultaneous mutations (GATA2-R398W, SETBP1, and ASXL1) were introduced into CD34$^+$ cells using CRISPR/Cas9 and rAAV6-GATA2^{R398W}-EGFP. Four days post-nucleofection, GFP$^+$ and GFP$^-$ cells were FACS-sorted for downstream in vitro studies. **B** In vitro expansion of liquid cultures initially seeded with control, GATA2-GFP$^+$, GATA2-GFP$^-$, multiplex-GFP$^+$ and multiplex-GFP$^-$ in fold increase ($n \geq 6$); Student's *t* test and Mann–Whitney U test. **C** Clonogenic (CFU) potential of control, GATA2-GFP$^+$, GATA2-GFP$^-$, multiplex-GFP$^+$ and multiplex-GFP$^-$ in primary and secondary replating ($n \geq 4$); Student's *t* test and Mann–Whitney U test. **D** Percentage of CD34$^+$ cells after 14 days in vitro ($n \geq 4$); Student's *t* test and Mann–Whitney U test. **E** Cell cycle analysis at day 14 for control, GATA2-GFP$^+$, GATA2-GFP$^-$, multiplex-GFP$^+$ and multiplex-GFP$^-$ ($n = 3$); Student's *t* test. **F** Apoptotic percentage at day 14 for control, GATA2-GFP$^+$, GATA2-GFP$^-$, multiplex-GFP$^+$ and multiplex-GFP$^-$ by Annexin-V staining ($n \geq 3$). **G** Percentage of mitotic cells quantified by semiautomatic analysis of large sets of high-resolution images at day 7. Between 50,000 to 150,000 cells were scored; Mann–Whitney U test. **H** Left panel shows representative images of normal mitotic phases and common mitotic defects by immunofluorescence. CellMask DR (red) was used to stain cell membranes, DAPI (blue) was used for DNA. Images were taken in the Opera Phenix. Right panel shows the percentage of mitotic defects in control and GATA2-GFP$^+$ in more than 50,000 analyzed cells at day 7; Student's *t* test; Scale bar = 10 μm. All data represent mean ± SEM. *$p < 0.05$; **$p < 0.01$, ***$p < 0.001$, ****$p < 0.0001$.

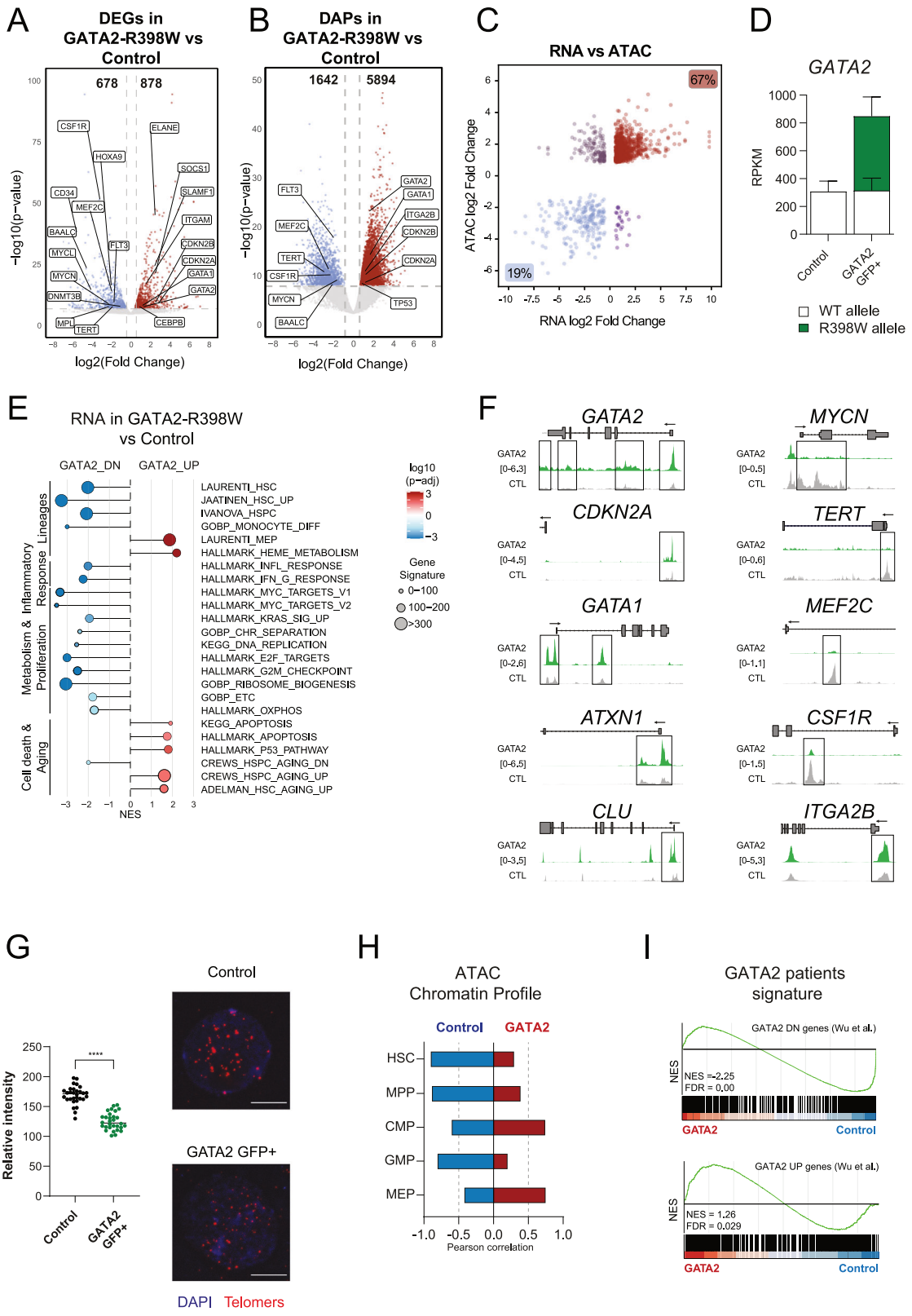

(Fig. 3G). GATA2-mutant cells showed a two-fold increase in mitotic abnormalities compared to controls, predominantly characterized by the presence of chromosome bridges, lagging chromosomes, multipolar spindles, and a significant increase in chromosome misalignments ($n > 1000$ mitotic cells analyzed) (Fig. 3H). Our data are in line with previously findings where GATA2 functions as a mitotic bookmark [38] and reveals a new role in mitosis regulation. These defects point to compromised mitotic fidelity and suggest that the GATA2-R398W mutation disrupts critical mechanisms of cell division, potentially

Fig. 4 GATA2-R398W mutation leads to chromatin and transcriptomic changes. A Volcano plot displaying gene expression changes, with log2 fold change on the x-axis and −log10 (p-value) on the y-axis. Dashed lines indicate thresholds for significance: p-adj = 0.05 and |log2 fold change| > 0.5: Relevant differentially expressed genes (DEGs) are labeled. **B** Volcano plot displaying chromatin accessibility changes, with log2 fold change on the x-axis and −log10 (p-value) on the y-axis. Dashed lines indicate thresholds for significance: p-adj = 0.05 and |log2 fold change| > 0.5. Relevant differentially accessible peaks (DAPs) are labeled. **C** Correlation analysis between DEGs and DAPs from RNA-seq and ATAC-seq data, demonstrating an 86% concordance between the two datasets. **D** Allele-specific expression (ASE) of wild-type (WT) and R398W *GATA2* in control and GATA2-GFP⁺ conditions from RNA-seq analysis. Data represent mean ± SEM. **E** Lollipop plot illustrating the Gene Set Enrichment Analysis (GSEA) for selected signatures on GATA2 vs control gene expression data. The dot size corresponds the number of genes belonging to the signature, the color gradient represents the adjusted p-value, and the x-axis reflects the Normalized Enrichment Score (NES) in GATA2-GFP$^+$ condition to control conditions. **F** ATAC-seq profiles showing representative chromatin accessibility regions in control (CTL) and GATA2-R398W-mutant cells. The squares highlight loci with increased accessibility (*GATA1*, *GATA2*, *ITGA2B*, *CDKN2A*, *CLU*, *ATXN1*) or decreased accessibility (*TERT*, *CSF1R*, *MEF2C*, *MYCN*) in GATA2-R398W cells compared to control. **G** Telomer length quantification of at least 30 nuclei by fluorescence in situ hybridization (FISH) in control and GATA2-R398W cells 7 days after sorter. Representative image obtained with Zeiss LSM880 confocal microscope equipped with AxioObserver Z1 inverted microscope. Telomers are label with Cy3 (red) and DNA with DAPI (blue); Student's *t* test; Scale bar = 10 μm. **H** Bar plot showing Pearson correlation values of normalized read counts for ATAC-seq peaks that overlap between control and GATA2-R398W cells and primary normal hematopoietic stem cell (HSC), multi-potent progenitor (MPP), common myeloid progenitor (CMP), and granulocyte-monocyte progenitor (GMP), megakaryocytic-erythroid progenitor (MEP) from Corces et al. [47]. **I** Graphical representation of the GSEA for a select group of genes that are upregulated (UP) or downregulated (DN) in GATA2 patients [39] ****$p < 0.0001$.

contributing to genomic instability and further leading to HSPCs exhaustion.

Transcriptomics and chromatin accessibility analysis of GATA2-R398W-mutant cells reveal a pre-aging phenotype

To identify dysregulated pathways in GATA2-mutant cells we performed transcriptomic (RNA-seq) and chromatin accessibility analysis (Assay for Transposase-Accessible Chromatin; ATAC-seq) of sorted GATA2-R398W GFP$^+$ cells at day ten of liquid culture comparing them to control unedited cells. We identified 678 downregulated and 878 upregulated significant differentially expressed genes (DEGs) (Table S2), along with 1642 regions of decreased and 5894 regions of increased chromatin accessibility (differentially accessible peaks, DAPs) (Table S3), in GATA2-mutant cells relative to control (Fig. 4A, B). A correlation analysis was performed using all the DEGs and DAPs. This analysis revealed a strong concordance between transcriptional and chromatin accessibility changes with a total of 86% (67% up and 19% down) correlation between RNA-seq and ATAC-seq profiles (Fig. 4C). Notably, *GATA2* gene expression increased by approximately 2.5-fold in GATA2-R398W-mutant GFP$^+$ cells, primarily driven by overexpression of the mutant R398W allele, rather than the wild-type (Fig. 4D). This observation is consistent with previously published studies [23, 35, 39, 40].

Gene Set Enrichment Analysis (GSEA) revealed downregulation of pathways associated with HSC maintenance, including genes such as *CD34, PROM1, SPINK2, HOXA9 and FLT3* (Fig. 4E; Fig. S4A). This data is consistent with the observed loss of the CD34$^+$ cells in vitro (Fig. 3). Conversely, genes associated with the megakaryocyte-erythroid progenitor (MEP) lineage, such as *GATA1*, *ITGA2B*, *EPOR,* and *NFE2*, were upregulated, indicating a shift in lineage priming (Fig. S4A). Moreover, genes associated with proliferation and chromosome segregation were downregulated, including *TERT*, its regulators (*MYCN*, *HMGA2*, *HMGB3*, *MXD1*) and other key genes (e.g., *MYCL, STARD9, and CEP68*). Additionally, key genes involved in cell cycle inhibition, *CDKN2A* (p16INK4A), *CDKN2B* (p15INK4B), *CDKN2D* (p19INK4D), were upregulated in GATA2-R398W cells (Fig. 4E; Fig. S4A). These findings might explain the impaired cell cycle progression and loss of stemness observed in GATA2-mutant cells in vitro (Fig. 3). Finally, the GSEA revealed an enrichment of pathways related to p53 signaling, apoptosis, and cellular aging in GATA2-mutant cells, including genes such as *CLU*, *ATXN1*, *CEBPB* and *SOCS1* (Fig. 4E; Fig. S4A) [41–44], suggesting activation of cellular stress responses. To evaluate whether the GATA2-R398W-mutant protein directly contributes to the transcriptional changes observed in our model, we intersected our list of DEGs with a publicly GATA2 chromatin immunoprecipitation sequencing (ChIP-seq) dataset [45, 46]. This approach allowed us to assess which of the dysregulated genes are direct targets of GATA2. Notably 64% of the upregulated and 58% of the downregulated genes were GATA2 targets (Fig. S4B). Key examples such as *CD34, HOXA9, FLT3, SPINK2, MYCL, CDKN2A, CDKN2B, STARD9, CEP68*, etc. are underscored in Fig. S4A, highlighting the significant involvement of GATA2 in the regulation of these transcripts.

These transcriptomic changes were corroborated at the chromatin level. GATA2-R398W cells exhibited increased chromatin accessibility at loci associated with *GATA1, GATA2, ITGA2B, CDKN2A, CLU* and *ATXN* while showing reduced accessibility at *TERT, CSF1R, MEF2C* and *MYCN* (Fig. 4F). To validate the downregulation of *TERT* observed at both the transcriptomic and chromatin levels, we performed fluorescence in situ hybridization (FISH) analysis to assess telomere length in GATA2-R398W GFP$^+$ cells. These analyses revealed a reduction in telomere signal intensity compared to control cells, strongly suggesting impaired telomere maintenance in GATA2-mutant cells (Fig. 4G).

Furthermore, the observed HSC/MEP transcriptional phenotype was validated by comparing our ATAC-seq data with published chromatin accessibility profiles of primary human hematopoietic populations [47]. This analysis revealed that the chromatin landscape of GATA2-R398W cells closely resembled that of MEP cells, in contrast to control cells, which more closely matched HSC/MPP and GMP populations (Fig. 4H). We next evaluated the predicted activity of transcription factors (TF) using DiffTF, based on chromatin accessibility peaks and TF binding motifs from the HOmo sapiens COmprehensive MOdel COllection (HOCOMOCO) database. Out of 766 TF analyzed, 228 binding sites were differentially accessible (FDR < 0.1) between control and GATA2-mutant cells. Of these, 107 sites exhibited downregulated activity, while 121 showed upregulated activity. In agreement with our RNA and published data [35], key transcription factor family motifs associated with hematopoiesis and proliferation (including GFI1B, IRF, MEIS, SPI, MYC) were downregulated. Conversely, increased activity was observed at motifs for the GATA2, SP, and CEBP transcription factor families (Fig. S4C).

Finally, to further validate our data we integrated our transcriptomic dataset with published data from BM-derived CD34$^+$ cells of GATA2 patients. A pseudobulk matrix [39] was generated from the single-cell RNA data to enable direct comparison. Interestingly we observed that our GATA2-mutant cells clustered together with GATA2-mutant patient cells (Fig. S4D). Additionally, we used the DEG list from GATA2 patients compared to healthy donors to define GATA2-Up and GATA2-Down signature gene set. GSEA revealed that our GATA2-mutant cells were significantly enriched for the GATA2-Up, whereas our control

cells were enriched for the GATA2-Down, recapitulating transcriptional patterns observed in GATA2-deficient patients (Fig. 4I).

Overall, these findings indicate that GATA2-R398W drives chromatin and transcriptional changes associated with reduced proliferative and mitotic activity and the activation of aging–related signatures, in line with the in vitro observations.

DISCUSSION

We developed a humanized model using CRISPR/Cas9-edited CB CD34⁺ cells with the GATA2-R398W mutation, alone and combined with SETBP1 and ASXL1 mutations, enabling detailed phenotypic, functional, and transcriptional analyses. In vivo expansion of edited clones through serial transplantation resulted in multilineage reconstitution and clonal selection of specific genetic combinations. Notably, our transplant model constitutes a competitive assay in which wild-type cells, GATA2-mutant cells, and cells harboring oncogenic somatic mutations compete. We observed a reduced fitness of GATA2-mutant cells compared to the wild-type cells, a disadvantage that persisted even in the presence of co-occurring mutations in SETBP1 and/or ASXL1. These findings highlight a cell intrinsic defect conferred by GATA2 mutation. Clinically, this observation is particularly relevant, as patients with germline GATA2 mutations lack a wild-type counterpart. Our data provide a compelling rationale for therapeutic gene editing approaches, whereby correction of GATA2 in a subset of HSPCs may endow those cells with a selective advantage, enabling them to outcompete mutant clones and potentially restore normal hematopoiesis.

Our in vitro analyses reveal important novel observations regarding the role of GATA2-R398W mutation in human CD34⁺ cells. First, we demonstrated that the GATA2-R398W mutation leads to pronounced mitotic defects in HSPCs. While previous work has highlighted the role of GATA2 as a mitotic bookmark [38], our findings go further by showing that the R398W mutation not only might disrupt mitotic chromatin retention but also impairs the mitotic process itself suggesting a direct role on chromosome segregation and genome maintenance. This novel insight supports a link between GATA2 protein dysfunction and mitotic instability, leading to compromised proliferative capacity of CD34⁺ cells, and potentially contributing to the reduced hematopoietic fitness in vivo. Future work will explore the mechanisms behind GATA2 mitotic role and disease progression.

Previous studies have suggested that allele-specific expression (ASE) affects GATA2 deficiency phenotype [17, 35, 40, 48]. Moreover, Hasegawa et al. [17] using an elegant mouse model of R398W mutation demonstrated that elevated levels of mutant GATA2 protein can exert dominant-negative effects, impairing wild-type GATA2 function and leading to cytopenia. Consistent with these findings, our transcriptomics revealed mutant allele upregulation in GATA2-R398W cells, linked to impaired proliferation and a pre-aging phenotype.

We observed a downregulation of MYC family members (*MYCN, MYCL*) which are essential regulators of proliferation [49, 50] and the upregulation of *CDKN2A* (p16), *CDKN2B* (p15), and *CDKN2D* (p19), key inhibitors of CDK4/6 that block the G1/S transition and tightly associated with cell cycle regulation [51, 52]. Most interestingly, in our GATA2-edited cells, we observed downregulation of known GATA2 targets that act as positive regulators of *TERT*, including the chromatin architectural proteins *HMGA2* [53, 54] and *HMGB3* [55], along with upregulation of the *TERT* repressor *JARID2* [56]. Based on these findings, we hypothesize that GATA2 mutations lead to dysregulation of TERT regulators, resulting in decreased *TERT* expression at both the transcriptomic and chromatin levels, ultimately contributing to telomere shortening. Although reduction of telomers length is frequently observed in patients with inherited BMF syndromes [57] it would be interesting to determine whether preventing or reversing telomere shortening could benefit GATA2-deficient cells.

In line with mitotic defects, we also observed the downregulation of *CEP68* and *STARD9*, which are essential for centrosome integrity and proper mitotic spindle formation. Disruption of these genes is known to cause chromosome missegregation and mitotic arrest or apoptosis [58, 59].

Collectively, these dysregulations give rise to a phenotype reminiscent of HSPC aging and exhaustion. Supporting this, we observed increased expression of aging-associated markers such as *CLU, SOCS, GATA1, ITGA2B* (*CD41*), and *SLAMF1*(*CD150*), in line with previous reports describing similar profiles in aged HSPCs [35, 41, 43, 60, 61]. Furthermore, similar transcriptional profiles were recently reported in two independent GATA2-R396Q mouse models [34, 35]. Most importantly, our transcriptomic data closely mirror gene expression patterns observed in CD34⁺ cells from GATA2-deficient patients, highlighting the clinical relevance and translational value of our model. These findings together with recent studies demonstrating mitochondrial dysfunction in GATA2-deficient cells [62] emphasize the complexity of GATA2 deficiency and its associated mutations.

Finally, emerging evidence suggests that CRISPR/Cas9/AAV6-mediated gene editing can activate senescence and inflammatory programs in edited HSPCs, potentially delaying, but not abolishing, their in vivo engraftment capacity [63]. In contrast, our in vitro and in vivo analyses consistently show a rapid and selective loss of GATA2-R398W-mutant cells within the first weeks following editing. Additionally, our transcriptomic profiling of GATA2-R398W-mutant cells revealed no upregulation of senescence or inflammatory signatures. These findings strongly suggests that the impaired fitness is not due to the editing process itself but rather is an intrinsic consequence of the *GATA2*-R398W mutation. Supporting this, in multiplex conditions, SETBP1- and ASXL1-mutant cells expanded efficiently despite similar AAV6 exposure, highlighting a selective disadvantage for GATA2-mutant HSPCs. The discrepancy from Conti et al. [63] may reflect timing of sample collection or targeted locus. Moreover, our transcriptomic analysis suggests that activation of the p53 pathway in our system may results as a downstream consequence of TERT downregulation, telomere shortening, and mitotic defects, ultimately leading to a pre-aging phenotype.

Our work highlights the feasibility of generating a human GATA2 deficiency model suitable for studying the biological consequences of various GATA2 variants and the generation of a platform for testing therapeutic compounds that might rescue their phenotype.

Limitations of the study

This study has some limitations. WES analysis was performed on bulk BM CD45⁺ cells, limiting clonal resolution and requiring VAF-based inference. The lack of clonal expansion in GATA2-mutant cells may be attributed to several factors. First, the absence of a mutant BM niche and a functional human immune system, both present in GATA2 patients. Second, GATA2 patients often suffer from chronic inflammation and recurrent infections, which may act as selective pressures driving clonal evolution. Lastly, our study focused on somatic mutations commonly associated with MDS, which typically require additional potent oncogenic hits, such as monosomy 7 or trisomy 8, for full leukemic transformation.

DATA AVAILABILITY

Bulk RNAseq and ATACseq data has been deposited in the National Center for Biotechnology Information's Gene Expression Omnibus with the following accession numbers: GSE282250 and GSE282251 respectively.

REFERENCES

1. Tsai FY, Keller G, Kuo FC, Weiss M, Chen J, Rosenblatt M, et al. An early haematopoietic defect in mice lacking the transcription factor GATA-2. Nature. 1994;371:221–6.
2. Dickinson RE, Griffin H, Bigley V, Reynard LN, Hussain R, Haniffa M, et al. Exome sequencing identifies GATA-2 mutation as the cause of dendritic cell, monocyte, B and NK lymphoid deficiency. Blood. 2011;118:2656–8.
3. Hahn CN, Chong CE, Carmichael CL, Wilkins EJ, Brautigan PJ, Li XC, et al. Heritable GATA2 mutations associated with familial myelodysplastic syndrome and acute myeloid leukemia. Nat Genet. 2011;43:1012–7.
4. Hsu AP, Sampaio EP, Khan J, Calvo KR, Lemieux JE, Patel SY, et al. Mutations in GATA2 are associated with the autosomal dominant and sporadic monocytopenia and mycobacterial infection (MonoMAC) syndrome. Blood. 2011;118:2653–5.
5. Ostergaard P, Simpson MA, Connell FC, Steward CG, Brice G, Woollard WJ, et al. Mutations in GATA2 cause primary lymphedema associated with a predisposition to acute myeloid leukemia (Emberger syndrome). Nat Genet. 2011;43:929–31.
6. Wlodarski MW, Hirabayashi S, Pastor V, Stary J, Hasle H, Masetti R, et al. Prevalence, clinical characteristics, and prognosis of GATA2-related myelodysplastic syndromes in children and adolescents. Blood. 2016;127:1387–97.
7. Largeaud L, Collin M, Monselet N, Vergez F, Fregona V, Larcher L, et al. Somatic genetic alterations predict haematological progression in GATA2 deficiency. Haematologica. 2023;108:1515.
8. Bodor C, Renneville A, Smith M, Charazac A, Iqbal S, Etancelin P, et al. Germ-line GATA2 p.THR354MET mutation in familial myelodysplastic syndrome with acquired monosomy 7 and ASXL1 mutation demonstrating rapid onset and poor survival. Haematologica. 2012;97:890–4.
9. West RR, Hsu AP, Holland SM, Cuellar-Rodriguez J, Hickstein DD. Acquired ASXL1 mutations are common in patients with inherited GATA2 mutations and correlate with myeloid transformation. Haematologica. 2014;99:276–81.
10. Donadieu J, Lamant M, Fieschi C, de Fontbrune FS, Caye A, Ouachee M, et al. Natural history of GATA2 deficiency in a survey of 79 French and Belgian patients. Haematologica. 2018;103:1278–87.
11. Kozyra EJ, Pastor VB, Lefkopoulos S, Sahoo SS, Busch H, Voss RK, et al. Synonymous GATA2 mutations result in selective loss of mutated RNA and are common in patients with GATA2 deficiency. Leukemia. 2020;34:2673–87.
12. Sahoo SS, Pastor VB, Goodings C, Voss RK, Kozyra EJ, Szvetnik A, et al. Clinical evolution, genetic landscape and trajectories of clonal hematopoiesis in SAMD9/SAMD9L syndromes. Nat Med. 2021;27:1806–17.
13. Marin-Bejar O, Romero-Moya D, Rodriguez-Ubreva J, Distefano M, Lessi F, Aretini P, et al. Epigenome profiling reveals aberrant DNA methylation signature in GATA2 deficiency. Haematologica. 2023;108:2551–7.
14. Romero-Moya D, Pera J, Marin-Bejar O, Torralba-Sales E, Murillo-Sanjuan L, Diaz-de-Heredia C, et al. Multiple phenotypes and epigenetic profiles in a three-generation family history with GATA2 deficiency. Leukemia. 2025;39:962–6.
15. Kotmayer L, Kozyra EJ, Kang G, Strahm B, Yoshimi A, Sahoo SS, et al. Age-dependent phenotypic and molecular evolution of pediatric MDS arising from GATA2 deficiency. Blood Cancer J. 2025;15:121.
16. Chong CE, Venugopal P, Stokes PH, Lee YK, Brautigan PJ, Yeung DTO, et al. Differential effects on gene transcription and hematopoietic differentiation correlate with GATA2 mutant disease phenotypes. Leukemia. 2018;32:194–202.
17. Hasegawa A, Hayasaka Y, Morita M, Takenaka Y, Hosaka Y, Hirano I, et al. Heterozygous variants in GATA2 contribute to DCML deficiency in mice by disrupting tandem protein binding. Commun Biol. 2022;5:376.
18. Pastor V, Hirabayashi S, Karow A, Wehrle J, Kozyra EJ, Nienhold R, et al. Mutational landscape in children with myelodysplastic syndromes is distinct from adults: specific somatic drivers and novel germline variants. Leukemia. 2017;31:759–62.
19. Mahony CB, Copper L, Vrljicak P, Noyvert B, Constantinidou C, Browne S, et al. Lineage skewing and genome instability underlie marrow failure in a zebrafish model of GATA2 deficiency. Cell Rep. 2023;42:112571.
20. Dobrzycki T, Mahony CB, Krecsmarik M, Koyunlar C, Rispoli R, Peulen-Zink J, et al. Deletion of a conserved Gata2 enhancer impairs haemogenic endothelium programming and adult Zebrafish haematopoiesis. Commun Biol. 2020;3:71.
21. Avagyan S, Weber MC, Ma S, Prasad M, Mannherz WP, Yang S, et al. Single-cell ATAC-seq reveals GATA2-dependent priming defect in myeloid and a maturation bottleneck in lymphoid lineages. Blood Adv. 2021;5:2673–86.
22. Gioacchino E, Koyunlar C, Zink J, de Looper H, de Jong M, Dobrzycki T, et al. Essential role for Gata2 in modulating lineage output from hematopoietic stem cells in zebrafish. Blood Adv. 2021;5:2687–700.
23. Gioacchino E, Zhang W, Koyunlar C, Zink J, de Looper H, Gussinklo KJ, et al. GATA2 heterozygosity causes an epigenetic feedback mechanism resulting in myeloid and erythroid dysplasia. Br J Haematol. 2024;205:580–93.
24. Ling KW, Ottersbach K, van Hamburg JP, Oziemlak A, Tsai FY, Orkin SH, et al. GATA-2 plays two functionally distinct roles during the ontogeny of hematopoietic stem cells. J Exp Med. 2004;200:871–82.
25. Rodrigues NP, Janzen V, Forkert R, Dombkowski DM, Boyd AS, Orkin SH, et al. Haploinsufficiency of GATA-2 perturbs adult hematopoietic stem-cell homeostasis. Blood. 2005;106:477–84.
26. Gao X, Johnson KD, Chang YI, Boyer ME, Dewey CN, Zhang J, et al. Gata2 cis-element is required for hematopoietic stem cell generation in the mammalian embryo. J Exp Med. 2013;210:2833–42.
27. de Pater E, Kaimakis P, Vink CS, Yokomizo T, Yamada-Inagawa T, van der Linden R, et al. Gata2 is required for HSC generation and survival. J Exp Med. 2013;210:2843–50.
28. Menendez-Gonzalez JB, Vukovic M, Abdelfattah A, Saleh L, Almotiri A, Thomas LA, et al. Gata2 as a crucial regulator of stem cells in adult hematopoiesis and acute myeloid leukemia. Stem Cell Rep. 2019;13:291–306.
29. Fernandez-Orth J, Koyunlar C, Weiss JM, Gioacchino E, de Looper H, Andrieux G, et al. Hematological phenotypes in GATA2 deficiency syndrome arise from aging, maladaptation to proliferation, and somatic events. Blood Adv. 2025;9:2794–807.
30. Johnson KD, Hsu AP, Ryu MJ, Wang J, Gao X, Boyer ME, et al. Cis-element mutated in GATA2-dependent immunodeficiency governs hematopoiesis and vascular integrity. J Clin Investig. 2012;122:3692–704.
31. Mehta C, Johnson KD, Gao X, Ong IM, Katsumura KR, McIver SC, et al. Integrating enhancer mechanisms to establish a hierarchical blood development program. Cell Rep. 2017;20:2966–79.
32. You X, Zhou Y, Chang YI, Kong G, Ranheim EA, Johnson KD, et al. Gata2 +9.5 enhancer regulates adult hematopoietic stem cell self-renewal and T-cell development. Blood Adv. 2022;6:1095–9.
33. Fu YK, Tan Y, Wu B, Dai YT, Xu XG, Pan MM, et al. Gata2-L359V impairs primitive and definitive hematopoiesis and blocks cell differentiation in murine chronic myelogenous leukemia model. Cell Death Dis. 2021;12:568.
34. Hall T, Mehmood R, Sa da Bandeira D, Cotton A, Klein J, Pruett-Miller SM, et al. Modeling GATA2 deficiency in mice: the R396Q mutation disrupts normal hematopoiesis. Leukemia. 2025;39:734–47.
35. Largeaud L, Fregona V, Jamrog LA, Hamelle C, Dufrechou S, Prade N, et al. GATA2 mutated allele specific expression is associated with a hyporesponsive state of HSC in GATA2 deficiency syndrome. Blood Cancer J. 2025;15:7.
36. Jung M, Cordes S, Zou J, Yu SJ, Guitart X, Hong SG, et al. GATA2 deficiency and human hematopoietic development modeled using induced pluripotent stem cells. Blood Adv. 2018;2:3553–65.
37. Marin-Bejar O, Pera J, Romero-Moya D, Torralba-Sales E, Distefano M, Giorgetti A. Human iPSCs-based modeling unveils chromatin remodeling induced by SETBP1 mutation as a potential initiating factor in GATA2 deficiency. Res Square. 2024 https://doi.org/10.21203/rs.3.rs-4984522/v1.
38. Silverio-Alves R, Kurochkin I, Rydstrom A, Vazquez Echegaray C, Haider J, Nicholls M, et al. GATA2 mitotic bookmarking is required for definitive haematopoiesis. Nat Commun. 2023;14:4645.
39. Wu Z, Gao S, Diamond C, Kajigaya S, Chen J, Shi R, et al. Sequencing of RNA in single cells reveals a distinct transcriptome signature of hematopoiesis in GATA2 deficiency. Blood Adv. 2020;4:2656–70.
40. Mulet-Lazaro R, van Herk S, Erpelinck C, Bindels E, Sanders MA, Vermeulen C, et al. Allele-specific expression of GATA2 due to epigenetic dysregulation in CEBPA double-mutant AML. Blood. 2021;138:160–77.
41. Chambers SM, Shaw CA, Gatza C, Fisk CJ, Donehower LA, Goodell MA. Aging hematopoietic stem cells decline in function and exhibit epigenetic dysregulation. PLoS Biol. 2007;5:e201.
42. Rossi DJ, Bryder D, Weissman IL. Hematopoietic stem cell aging: mechanism and consequence. Exp Gerontol. 2007;42:385–90.
43. Adelman ER, Huang HT, Roisman A, Olsson A, Colaprico A, Qin T, et al. Aging human hematopoietic stem cells manifest profound epigenetic reprogramming of enhancers that may predispose to leukemia. Cancer Discov. 2019;9:1080–101.
44. Flohr Svendsen A, Yang D, Kim K, Lazare S, Skinder N, Zwart E, et al. A comprehensive transcriptome signature of murine hematopoietic stem cell aging. Blood. 2021;138:439–51.
45. Fujiwara T, O'Geen H, Keles S, Blahnik K, Linnemann AK, Kang YA, et al. Discovering hematopoietic mechanisms through genome-wide analysis of GATA factor chromatin occupancy. Mol Cell. 2009;36:667–81.
46. Castano J, Aranda S, Bueno C, Calero-Nieto FJ, Mejia-Ramirez E, Mosquera JL, et al. GATA2 promotes hematopoietic development and represses cardiac differentiation of human mesoderm. Stem Cell Rep. 2019;13:515–29.
47. Corces MR, Buenrostro JD, Wu B, Greenside PG, Chan SM, Koenig JL, et al. Lineage-specific and single-cell chromatin accessibility charts human hematopoiesis and leukemia evolution. Nat Genet. 2016;48:1193–203.
48. Al Seraihi AF, Rio-Machin A, Tawana K, Bodor C, Wang J, Nagano A, et al. GATA2 monoallelic expression underlies reduced penetrance in inherited GATA2-mutated MDS/AML. Leukemia. 2018;32:2502–7.
49. Eilers M. Control of cell proliferation by Myc family genes. Mol Cells. 1999;9:1–6.
50. Yar MS, Haider K, Gohel V, Siddiqui NA, Kamal A. Synthetic lethality on drug discovery: an update on cancer therapy. Expert Opin Drug Discov. 2020;15:823–32.

51. Iolascon A, Giordani L, Moretti A, Tonini GP, Lo Cunsolo C, Mastropietro S, et al. Structural and functional analysis of cyclin-dependent kinase inhibitor genes (CDKN2A, CDKN2B, and CDKN2C) in neuroblastoma. Pediatr Res. 1998;43:139–44.
52. Arcellana-Panlilio MY, Egeler RM, Ujack E, Pinto A, Demetrick DJ, Robbins SM, et al. Decreased expression of the INK4 family of cyclin-dependent kinase inhibitors in Wilms tumor. Genes Chromosomes Cancer. 2000;29:63–9.
53. Li AY, Lin HH, Kuo CY, Shih HM, Wang CC, Yen Y, et al. High-mobility group A2 protein modulates hTERT transcription to promote tumorigenesis. Mol Cell Biol. 2011;31:2605–17.
54. Natarajan S, Begum F, Gim J, Wark L, Henderson D, Davie JR, et al. High mobility group A2 protects cancer cells against telomere dysfunction. Oncotarget. 2016;7:12761–82.
55. Li Z, Zhang Y, Sui S, Hua Y, Zhao A, Tian X, et al. Targeting HMGB3/hTERT axis for radioresistance in cervical cancer. J Exp Clin Cancer Res. 2020;39:243.
56. Graham MK, Xu B, Davis C, Meeker AK, Heaphy CM, Yegnasubramanian S, et al. The TERT Promoter is polycomb-repressed in neuroblastoma cells with long telomeres. Cancer Res Commun. 2024;4:1533–47.
57. Townsley DM, Dumitriu B, Liu D, Biancotto A, Weinstein B, Chen C, et al. Danazol treatment for telomere diseases. N Engl J Med. 2016;374:1922–31.
58. Graser S, Stierhof YD, Nigg EA. Cep68 and Cep215 (Cdk5rap2) are required for centrosome cohesion. J Cell Sci. 2007;120:4321–31.
59. Torres JZ, Summers MK, Peterson D, Brauer MJ, Lee J, Senese S, et al. The STARD9/Kif16a kinesin associates with mitotic microtubules and regulates spindle pole assembly. Cell. 2011;147:1309–23.
60. Gekas C, Graf T. CD41 expression marks myeloid-biased adult hematopoietic stem cells and increases with age. Blood. 2013;121:4463–72.
61. Bernitz JM, Kim HS, MacArthur B, Sieburg H, Moore K. Hematopoietic stem cells count and remember self-renewal divisions. Cell. 2016;167:1296–309.e10.
62. Rein A, Geron I, Kugler E, Fishman H, Gottlieb E, Abramovich I, et al. Cellular and metabolic characteristics of pre-leukemic hematopoietic progenitors with GATA2 haploinsuficiency. Haematologica. 2022;108:2316.
63. Conti A, Giannetti K, Midena F, Beretta S, Gualandi N, De Marco R, et al. Senescence and inflammation are unintended adverse consequences of CRISPR-Cas9/AAV6-mediated gene editing in hematopoietic stem cells. Cell Rep Med. 2025;6:102157

ACKNOWLEDGEMENTS

This work was supported by ERA PerMed GATA2-HuMo Funding Mechanism (Spain: Acció Instrumental de SLT011/18/00006 of the Department of Health of the Government of Catalonia), Ministerio de Ciencia e Innovación, which is part of Agencia Estatal de Investigación (AEI), through the Retos Investigación grant, number PID2020-115591RB-I00/ https://doi.org/10.13039/501100011033, and PID2023-146290OB-I00, Fundació La Marató TV3 228/C/2020, Award no. AC23_2/00040 by ISCIII through AES 2023 and within the European Joint Programme Rare Diseases framework, Instituto de Salud Carlos III (ISCIII), "Programa FORTALECE del Ministerio de Ciencia e Innovación", through the project number FORT23/00032 and Finançat per el Departament de Recerca i Universitats de la Generalitat de Catalunya i l'AGAUR (expedient 2021 SGR 00888) to AG. Funding for this project was provided in part by an EHA Research Grant award granted by the European Hematology Association (KOG-202109-01162) and the European Union's Horizon 2020 research and innovation programme under the Marie Sklodowska-Curie grant agreement No 101029927 to OM-B. DR-M was supported by Deutsche José Carreras Leukämie-Stiftung, DJCLS 13 R/2022. JP and MD were supported by Fundació La Marató TV3 228/C/2020. MM-M was supported by the TC030-AND/2022 Predoctoral grant from the Government of Andorra. OM-B is currently supported by the Ramón y Cajal contract (RYC2021-032129-I) funded by AEI/European Social Fund UE. The work in the LP laboratory was supported by "la Caixa" Foundation, LCF-PR-HR24-00150 and by PID2023-151556OB-I00 and CNS2024-154742 funded by MICIU/AEI/10.13039/501100011033 and, as appropriate, by "ESF Investing in your future", by "ESF + " or by "European Union NextGenerationEU/PRTR". The work in AB laboratory was funded by ERA PerMed-Departament de Salut, Generalitat de Catalunya (SLT011/18/00007) and the EJP RD-Instituto de Salud Carlos III (AC23_2/00014). The work of CC and OM was supported by the Spanish Ministry of Economy and Competitiveness/European Union NextGenerationEU (PID2022-142966OB-I00) and the Deutsche José Carreras Leukämie-Stifttung (DJCLS 15 R/2023) to OM. CC is supported by a predoctoral fellowship from the Spanish Ministry of Economy and Competitiveness (PID2022-1429660B-100). The work of MP was supported by a Ramón y Cajal contract of the Spanish Ministry of Science, Innovation and Universities (Grant: RYC2018-024564-I funded by MICIU/AEI /10.13039/501100011033 and by "El FSE invierte en tu futuro"). The work in the MP laboratory was supported by the project PID2022-139580OB-I00 funded by MICIU/AEI /10.13039/501100011033 and FEDER and by "ERDF A way of making Europe", by the European Union. MWW was supported by Evans MDS DRG grant and American Society of Hematology bridge award. Authors thank the members of the Advanced Optical Microscopy facility from UB (Scientific and Technological Centers, Universitat de Barcelona [CCiTUB]) for their technical support. We thank the CERCA Programme/Generalitat de Catalunya for institutional support.

AUTHOR CONTRIBUTIONS

DR-M and AG designed the study and wrote the manuscript. DR-M, CC, OM-B, MM, JP, JC, FdG, JG, AI, CB-B, performed cell biology experiments and data analysis. ETS, MD, MS performed bioinformatic analysis. MP, LP, AC, OM, MWW, AB, and AG supervised data analysis. All authors contributed to the manuscript and provided final approval.

COMPETING INTERESTS

The authors declare no conflicts of interest.

ETHICS APPROVAL AND CONSENT TO PARTICIPATE

All methods described in this manuscript were performed in accordance with the relevant guidelines and regulations. The animal experiments in this study have been approved by our Animal Ethics Committee of PRBB and are conducted in accordance with the regulation from the "Departament de Medi Ambient i Habitatge de la Generalitat de Catalunya" with the protocol number 10655; Ethics Committee on Animal Experimentation (CEEA): ABS-19-0045-P4. Healthy donors mobilized peripheral blood $CD34^+$ cells were obtained with written informed consent and approval of the Institutional Review Board (IRB) of Fred Hutchinson Cancer Research Center with the approval number #985.03. Cord blood units from healthy newborns were obtained from the Blood Tissue Bank following the institutional guidelines approved by the local IRB with the approval number 206-173-1. All patients or their guardians signed informed consents for sample collection in accordance with the Declaration of Helsinki.

ADDITIONAL INFORMATION

Supplementary information The online version contains supplementary material available at https://doi.org/10.1038/s41375-025-02771-8.

Correspondence and requests for materials should be addressed to Alessandra Giorgetti.

Reprints and permission information is available at http://www.nature.com/reprints

Publisher's note Springer Nature remains neutral with regard to jurisdictional claims in published maps and institutional affiliations.